Childs Nerv Syst (2015) 31:2277–2281
DOI 10.1007/s00381-015-2901-5

ORIGINAL PAPER

CSF flow pathways through the ventricle–cistern interfaces in kaolin-induced hydrocephalus rats—laboratory investigation

Jong-Seok Yoon[1] · **Taek-kyun Nam**[1] · **Jeong-taik Kwon**[1] · **Seung-won Park**[1] · **Yong-sook Park**[1]

Received: 1 July 2015 / Accepted: 1 September 2015 / Published online: 8 September 2015

Abstract
Purpose The goal of this study was to identify direct cerebrospinal fluid (CSF) pathways in the interface between ventricles and cisterns. Such routes are hypothesized to be involved in alternative CSF flows in abnormal circumstances of CSF circulation.
Methods Chronic obstructive hydrocephalus models were induced in ten Sprague–Dawley rats with kaolin injection into the cisterna magna. Three weeks after the kaolin injection, when thick arachnoid fibrosis obliterated the fourth ventricular outlets, cationized ferritin was stereotactically infused as a tracer into the lateral ventricle in order to observe the pathways from the ventricles to the subarachnoid space. Animals were killed in 48 h and brains were sectioned. CSF flow pathways were traced by the staining of ferritin with ferrocyanide.
Results Eight out of ten rats developed hydrocephalus. The subarachnoid membranes of the convexity and basal cisterns were severely adhered such that most of the ferritin remained in the ventricles whereas basal and convexity cisterns were clear of ferritin. In six out of the eight hydrocephalus rats, ferritin leaked from the third ventricle into the quadrigeminal cistern, and from the lateral ventricle into the ambient cistern.
Conclusions The interfaces between the third ventricle and the quadrigeminal cistern, and between the lateral ventricle and the ambient cistern appear to be alternative CSF pathways in a pathologic condition such as obstructive hydrocephalus.

✉ Yong-sook Park
cuttage@cau.ac.kr

[1] Department of Neurosurgery, Chung-Ang University Hospital, Heukseok-ro 102, Dongjak-gu, Seoul, Republic of Korea

Keywords Cerebrospinal fluid · CSF circulation · Hydrocephalus · Kaolin · Cerebral ventricle

Introduction

Circulation of cerebrospinal fluid (CSF) can be understood from the perspective of fluid dynamics. CSF flow comprises two different mechanisms. Bulk flow is driven by arteriovenous pressure gradients and arterial pulsations traversing the ventricular system in a caudal direction toward the brainstem apertures. From there, the subarachnoid CSF flow can be bidirectional: either descending to the spinal cord or ascending to the dorsal and rostral parts of the brain [1]. The laminar flow occurs only inside the ventricular system in a very thin layer along the walls in a variety of directions and is driven by the beating of cilia of local ependymal cells. Interruption of either the bulk or laminar flow results in hydrocephalus [2].

Contrary to this classical pathway, some studies have suggested that there are additional CSF pathways. In several animal experiments, peptides and other potentially neuroactive compounds have been administered into the ventricles and have been shown to affect CNS functions within minutes [3, 4]. In order to accomplish this, CSF flow must be fairly brisk and directed to the appropriate cerebral and cerebrovascular tissues. A study of intracranial distribution of an isotope revealed the appearance of the isotope in the velum interpositum before the fourth ventricles and the superior medullary velum before the basal cisterns [5]. Others have suggested that pressure gradients impact the dynamics of CSF flow. However, these pressure gradients have not been observed in humans with hydrocephalus or among ventricles, subarachnoid space, and brain tissues during the development of hydrocephalus in experimental models [6–9].

Existing evidence suggests that there may be alternative pathways of CSF circulation between ventricles and subarachnoid cisterns. These pathways may aid in maintaining pressure balance between cisterns and ventricles under a condition of increased intraventricular pressure. However, no study has directly examined alternative pathways. Accordingly, this study induced experimental conditions in which the foramens of the fourth ventricle and subarachnoid spaces were obliterated with kaolin in rat hydrocephalus models. A tracer was injected into a lateral ventricle and the CSF routes were observed microscopically.

Materials and methods

Chronic hydrocephalus model making with intraventricular ferritin injection

Ten non-conditioned, male adult Sprague–Dawley rats weighting between 280 and 300 g were used. They all had free access to rat chow and water. Cages were kept in a temperature- and humidity-controlled room with a 12-h light–dark cycle. Anesthesia was maintained with a peritoneal injection of a mixture of ketamine (60 μg/g) and rompun (4 mg/kg) throughout all surgical procedures. Surgeries were performed using sterile techniques with the rat in a prone position in a stereotactic frame.

The soft tissues of the posterior head and neck midline were incised to identify the craniocervical junction under microscopic guidance. A midline suboccipital craniectomy exposed the cisterna magna. After identifying the arachnoid membrane of the cisterna magna, a 30-gauge needle was inserted into the subarachnoid space and 100 μL of 20 % kaolin (aluminum silicate; Sigma, St. Louis, MO, USA) was injected into the cistern at the rate of about 6 μL/s. Microfibrillar collagen (Avitene®, Medchem Inc., MA., USA) was applied over the dorsal cisternal surface to prevent CSF leakage and hemostasis [10, 11]. The skin was then tightly closed. Three weeks after the surgery, intraventricular ferritin injection was performed. Rats were anesthetized in the same manner and fixed in a stereotactic frame. The skin over the cranium was incised and the junction of the sagittal and coronal sutures was identified. A small, high-speed microdrill with a rounded tip was used to grind away the bone to expose the dural membrane. The dural membrane around the point of needle entry was incised. Ventricular puncture coordinates were 1 mm posterior, 1.5 mm lateral to bregma, and 3.5 mm in depth. A 50-μL Hamilton syringe (Fisher Scientific, Toronto, ON, Canada) with a 30-gauge needle was used. Twenty microliters of cationized ferritin (Sigma Chemicals Co., St. Louis, MO, USA) was used as a tracer and was infused into the right lateral ventricle. Forty-eight hours after the intraventricular tracer injection, animals were deeply sedated with ketamine and transcardially perfused with 0.9 % saline and 4 % buffered paraformaldehyde. The brains were extracted and fixed in 4 % buffered paraformaldehyde by immersion in 5 mL of the solution for 2 h and then immersed in 0.1 M phosphate buffer (pH 7.4) containing 30 % sucrose for 24 h. The brain was then sliced coronally into 40-μm-thick sections using a freezing microtome and then stained with ferrocyanide [12]. All experimental procedures were performed in accordance with Chung-Ang University guidelines for the use and care of laboratory animals.

Sham operations with intraventricular ferritin injection

In five non-conditioned animals, the soft tissues of the posterior head and neck midline were incised to identify the craniocervical junction under microscopic guidance. A midline suboccipital craniectomy exposed the cisterna magna. After identifying the arachnoid membrane of the cisterna magna, 100 μL of saline was injected into the cistern. Three weeks post-surgery, 20 μL of ferritin was infused into the right lateral ventricle. All of these animals were killed within 48 h of the tracer injection and prepared for microscopic examination in the same manner as the case animals.

Measurement of ventricle size

Ventricular enlargement was measured using the Evans' index of the maximal width of the lateral ventricles divided by the maximal width of the brain on the coronal section at the level of the interventricular foramen.

Results

Anatomical assessments of kaolin-induced hydrocephalus

There was remarkable arachnoid adhesion in the olfactory bulbs, basal cisterns, cisterna magna, convexity cisterns, and spinal cisterns, including the spinal nerve roots. This is previously published as a comparative experimental model for acute versus chronic hydrocephalus [11]. On microscopic examination, kaolin particles were dispersed in the cisterns and induced fibrosis of the arachnoid membrane. The mean Evans' indices were 0.53±0.09 in eight out of the ten kaolin-induced hydrocephalus rats and 0.37±0.02 in the five sham animals.

Microscopic examinations

All ventricular walls were stained blue by the ferritin/ferrocyanide, and basal and convexity cisterns were clear of ferritin in kaolin-induced models. However, in the sham animals, all ventricles, and basal and convexity cisterns are stained blue

as expected. This confirms that the intraventricular injected tracer did not exit the fourth ventricular foramens or did not circulate to the basal and convexity cisterns in the experimental group. Nevertheless, the quadrigeminal cisterns on the side abutting the dorsal third ventricle were stained in six of the eight rats (Fig. 1). The source of ferritin in quadrigeminal cisterns appeared to originate from the third ventricle. The inner tissue of the velum interpositum above the third ventricular roof was not stained in any animals (Fig. 1).

Ambient cisterns on the side facing the temporal horn of the lateral ventricle were stained in six of the eight rats (Fig. 2) even though the basal cisterns were not stained. Ferritin appeared to exit from the temporal horns and move toward the basal cisterns, but it did not reach the basal side of the cisterns in which the kaolin particles had been deposited. The deposited kaolin and subsequent arachnoid inflammation appeared to prevent the further advancement of the tracer by passing through the basal cisterns.

Discussion

Experimental hydrocephalus can be induced by the injection of kaolin into the cisterna magna in a wide range of species. Ventricular enlargement occurs as a result of the inflammatory scarring, which causes an obstruction of the CSF pathways near the fourth ventricle outlets [13, 14].

Experimental evidences of being additional CSF flow pathways

Ghersi-Egea et al. [5] have suggested that there are additional CSF pathways. They used a time course, radio-labeled intracranial distribution of [^{14}C] sucrose in non-conditioned rats. When the tracer was injected into lateral ventricles, within 3.5 min the tracer appeared in the third ventricle, aqueduct of sylvius, velum interpositum, fourth ventricles, and superior medullary velum and, within 5 min, in the interpeduncular, ambient, and quadrigeminal cisterns. They presumed that this rapid appearance in the quadrigeminal cistern and ambient cistern is a convective delivery of sugar via the velum interpositum. They pointed out the velum interpositum and superior medullary velum seemed to be the passageways for the rapid flow of CSF-borne sucrose into the velae. The findings of the present study do not support this pathway, as we did not find any staining in the velum interpositum. The reason for this discrepancy remains unclear. However, it may be due to the molecular weights of sucrose (342 kDa) and ferritin (450 kDa) [15]. Smaller molecules may pass through the velum interpositum while larger ones do not. If it is so, CSF likely moves through this interface more easily than other molecules. If we had used a tracer with a smaller molecular weight, we may have been able to identify additional potential pathways. In a series of experiments involving respiratory and cardiovascular control mechanisms in cats, the effects of vasopressin administered into the lateral ventricle were observed within 2 min at the ventral surface of the brainstem [16]. A tracer of horseradish peroxidase administered into the lateral

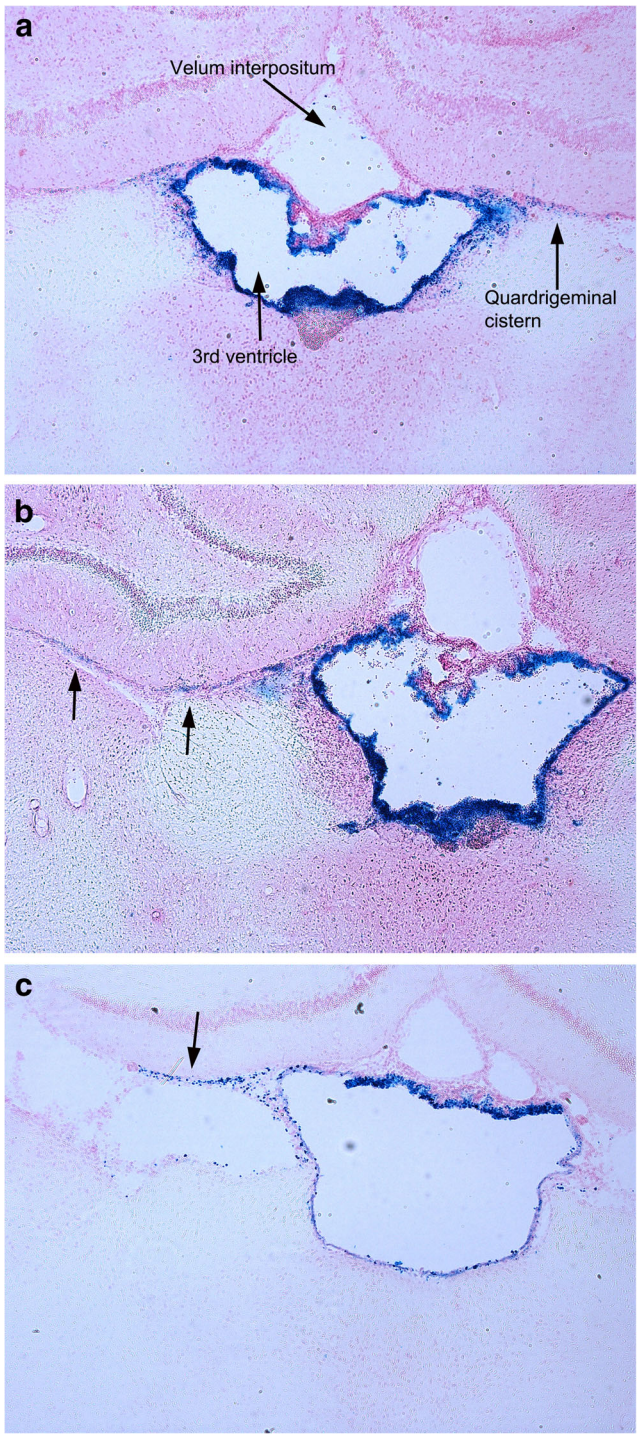

Fig. 1 Ferritin staining in the third ventricle and quadrigeminal cistern (**a**–**c**, ferrocyanide stain × 50). Quadrigeminal cisterns show linear staining in three different animals, and it seems to be leaked from the adjacent third ventricle. Velum interpositum is clear from ferritin

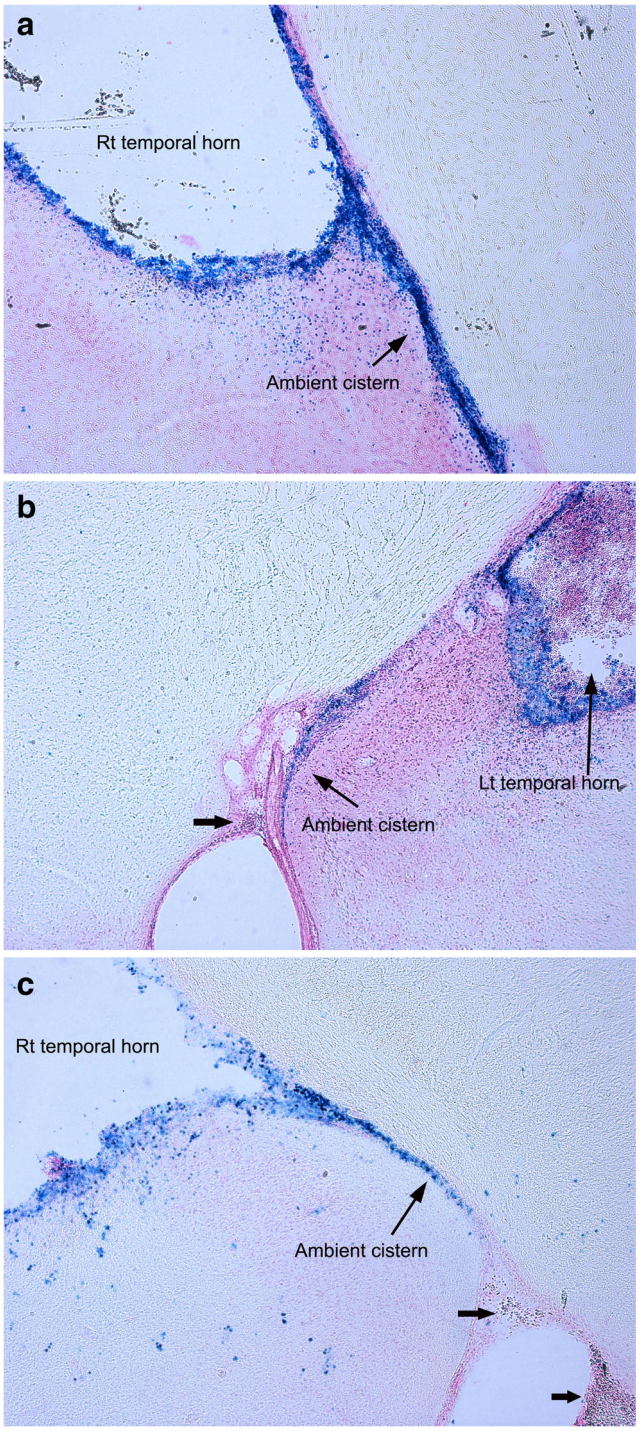

Fig. 2 Ferritin staining in the lateral ventricle and ambient cistern. Temporal horns of lateral ventricles are stained blue well and some spillage of tracer into ambient cisterns are noticed (**a**–**c**, ferrocyanide stain × 50). *Black block arrows* in (**b**) and (**c**) show deposition of kaolin particles in basal cistern. Ferritin in ambient cisterns (**b**, **c**) stopped just before the basal cisterns which adhered to each other and prevented farther advancement of CSF

ventricle of the cat penetrates the outer surface of the brainstem within 4 or 5 min [17]. Similarly, a rapid distribution of tracers such as [^{14}C]Inulin and [^{125}I]CRH after injection into the lateral ventricle has also been observed in rats [18].

Recent measurements of the pulsatile flow rates in the cerebral aqueduct of the human brain using modern imaging and other techniques revealed evidence of the high speed of this CSF transport channel [19–21]. Maximal flow rates of 12 mm/s and higher were observed in the aqueduct [22, 23], while at other sites such as the spinal canal, the flow rate was almost negligible [22]. Because of the fast velocity of CSF, it is possible that, under normal conditions, most CSF flows follow the known CSF pathways. However, in the case of increased intracranial pressure, the region from the third ventricle to the quadrigeminal cistern or from the lateral ventricle to the ambient cistern could be alternative pathways.

In the clinical condition such as arrested hydrocephalus, gradual obstruction of aqueduct by tectal masses, it does not always develop clinically hydrocephalus. We can carefully presume the ventricle–cistern interfaces may become bypass routes in these circumstances.

Some studies have attempted to identify the transmantle pressure gradients between each compartment of brain tissues under hydrocephalus [6–9]. However, when the intracranial pressure was measured at the ventricle, cisterna magna, convexity subarachnoid space, and the brain tissue and the sagittal sinus, all intracranial compartments including the sagittal sinus increased pressure simultaneously and achieved steady state pressure rapidly, regardless of fluid injection site [7]. The findings of the present study in conjunction with those of studies previously mentioned suggest that blockage of the traditional CSF pathway may open other pores to egress the accumulated CSF to equilibrate the intracranial pressure.

Bidirectional transport of CSF through the ventricles and cisterns?

In the previous experimental setting of CSF pathways, we demonstrated cistern to ventricular pathway in an acute form of hydrocephalus [10]. In the present study, the opposite direction is displayed. Considering these results, we reach a hypothesis that CSF in the ventricle and cistern can move bidirectionally from each compartment. Recent CSF studies suggested that the traditional concepts about CSF production, distribution, and absorption may have some misinterpretations [9, 24]. In the distribution of CSF, intracisternal injected ^{3}H-inulin was distributed to lateral ventricle [25] and lumbar injected methotrexate in patients reached therapeutic concentration in lateral ventricle [26]. The fundamental assumption is that this CSF distribution is caused by the pulsation and to-and-pro displacements and mixing of CSF volume [24]. They admit that CSF moves bidirectionally between cisterns and ventricles; however, the exact route was not mentioned. The present study may play some roles in this distribution in the CNS compartments.

Limitations of this study

We did not include the posterior fossa and surrounding structures in order to identify the potential pathways because these regions were manipulated at the time of model making; the superior medullar velum could be an additional potential pathway as Ghersi-Egea et al. illustrated. There is a possibility that other dormant routes occur between ventricles and cisterns. These pathways could be better identified using a molecule smaller than ferritin. The contribution of the quadrigeminal cistern and the ambient cistern to pressure balance or the volume of CSF flow should be quantified.

Future ultrastructural studies should investigate the exact points or areas of CSF communication between ventricles and cisterns. However, ependyma is demonstrated that it has discontinuous plaques known as gap junctions [27] and the gap junctions are present within the arachnoid trabecula layer and the arachnoid cells [28].

Conclusion

The interface between the third ventricle and the quadrigeminal cistern and between the lateral ventricle and ambient cistern may be alternative CSF pathways in hydrocephalus conditions. These interface may become a bidirectional route for CSF distribution in the brain.

References

1. Reiber H (2003) Proteins in cerebrospinal fluid and blood: barriers, CSF flow rate and source-related dynamics. Restor Neurol Neurosci 21:79–96
2. Nguyen T, Chin WC, O'Brien JA, Verdugo P, Berger AJ (2001) Intracellular pathways regulating ciliary beating of rat brain ependymal cells. J Physiol 531:131–140
3. Raichle ME, Grubb RL Jr (1978) Regulation of brain water permeability by centrally-released vasopressin. Brain Res 143:191–194
4. Rosenberg GA, Kyner WT, Fenstermacher JD, Patlak CS (1986) Effect of vasopressin on ependymal and capillary permeability to tritiated water in cat. Am J Physiol 251:F485–F489
5. Ghersi-Egea JF, Finnegan W, Chen JL, Fenstermacher JD (1996) Rapid distribution of intraventricularly administered sucrose into cerebrospinal fluid cisterns via subarachnoid velae in rat. Neuroscience 75:1271–1288
6. Penn RD, Lee MC, Linninger AA, Miesel K, Lu SN, Stylos L (2005) Pressure gradients in the brain in an experimental model of hydrocephalus. J Neurosurg 102:1069–1075
7. Shapiro K, Kohn IJ, Takei F, Zee C (1987) Progressive ventricular enlargement in cats in the absence of transmantle pressure gradients. J Neurosurg 67:88–92
8. Stephensen H, Tisell M, Wikkelso C (2002) There is no transmantle pressure gradient in communicating or noncommunicating hydrocephalus. Neurosurgery 50:763–771, discussion 771–763
9. Klarica M, Oreskovic D, Bozic B, Vukic M, Butkovic V, Bulat M (2009) New experimental model of acute aqueductal blockage in cats: effects on cerebrospinal fluid pressure and the size of brain ventricles. Neuroscience 158:1397–1405
10. Park JH, Park YS, Suk JS, Park SW, Hwang SN, Nam TK, Kim YB, Lee WB (2011) Cerebrospinal fluid pathways from cisterns to ventricles in N-butyl cyanoacrylate-induced hydrocephalic rats. J Neurosurg Pediatr 8:640–646
11. Park YS, Park SW, Suk JS, Nam TK (2011) Development of an acute obstructive hydrocephalus model in rats using N-butyl cyanoacrylate. Childs Nerv Syst 27:903–910
12. Parmley RT, Ostroy F, Gams RA, DeLucas L (1979) Ferrocyanide staining of transferrin and ferritin-conjugated antibody to transferrin. J Histochem Cytochem 27:681–685
13. Odake G, Yamaki T, Naruse S (1978) CSF-circulation pathways in experimental hydrocephalus of the rat (author's transl). Neurol Med Chir (Tokyo) 18:673–680
14. Hochwald GM (1985) Animal models of hydrocephalus: recent developments. Proc Soc Exp Biol Med 178:1–11
15. Theil EC (1987) Ferritin: structure, gene regulation, and cellular function in animals, plants, and microorganisms. Annu Rev Biochem 56:289–315
16. Feldberg W (1976) The ventral surface of the brain stem: a scarcely explored region of pharmacological sensitivity. Neuroscience 1: 427–441
17. Borison HL, Borison R, McCarthy LE (1980) Brain stem penetration by horseradish peroxidase from the cerebrospinal fluid spaces in the cat. Exp Neurol 69:271–289
18. Proescholdt MG, Hutto B, Brady LS, Herkenham M (2000) Studies of cerebrospinal fluid flow and penetration into brain following lateral ventricle and cisterna magna injections of the tracer [14C]inulin in rat. Neuroscience 95:577–592
19. McCormack EJ, Egnor MR, Wagshul ME (2007) Improved cerebrospinal fluid flow measurements using phase contrast balanced steady-state free precession. Magn Reson Imaging 25:172–182
20. Wagshul ME, Chen JJ, Egnor MR, McCormack EJ, Roche PE (2006) Amplitude and phase of cerebrospinal fluid pulsations: experimental studies and review of the literature. J Neurosurg 104: 810–819
21. Greitz D (1993) Cerebrospinal fluid circulation and associated intracranial dynamics. A radiologic investigation using MR imaging and radionuclide cisternography. Acta Radiol Suppl 386:1–23
22. Gupta S, Soellinger M, Boesiger P, Poulikakos D, Kurtcuoglu V (2009) Three-dimensional computational modeling of subject-specific cerebrospinal fluid flow in the subarachnoid space. J Biomech Eng 131:021010
23. Howden L, Giddings D, Power H, Aroussi A, Vloeberghs M, Garnett M, Walker D (2008) Three-dimensional cerebrospinal fluid flow within the human ventricular system. Comput Methods Biomech Biomed Engin 11:123–133
24. Vladic A, Klarica M, Bulat M (2009) Dynamics of distribution of 3H-inulin between the cerebrospinal fluid compartments. Brain Res 1248:127–135
25. Bulat M, Lupret V, Orehkovic D, Klarica M (2008) Transventricular and transpial absorption of cerebrospinal fluid into cerebral microvessels. Coll Antropol 32(Suppl 1):43–50
26. Shapiro WR, Young DF, Mehta BM (1975) Methotrexate: distribution in cerebrospinal fluid after intravenous, ventricular and lumbar injections. N Engl J Med 293:161–166
27. Brightman MW (1965) The distribution within the brain of ferritin injected into cerebrospinal fluid compartments. I. Ependymal distribution. J Cell Biol 26:99–123
28. Barshes N, Demopoulos A, Engelhard HH (2005) Anatomy and physiology of the leptomeninges and CSF space. Cancer Treat Res 125:1–16